NASA/TM—2013-216547

Simulating the Use of Alternative Fuels in a Turbofan Engine

Jonathan S. Litt and Jeffrey C. Chin
Glenn Research Center, Cleveland, Ohio

Yuan Liu
N&R Engineering, Inc., Parma Heights, Ohio

September 2013

NASA STI Program . . . in Profile

Since its founding, NASA has been dedicated to the advancement of aeronautics and space science. The NASA Scientific and Technical Information (STI) program plays a key part in helping NASA maintain this important role.

The NASA STI Program operates under the auspices of the Agency Chief Information Officer. It collects, organizes, provides for archiving, and disseminates NASA's STI. The NASA STI program provides access to the NASA Aeronautics and Space Database and its public interface, the NASA Technical Reports Server, thus providing one of the largest collections of aeronautical and space science STI in the world. Results are published in both non-NASA channels and by NASA in the NASA STI Report Series, which includes the following report types:

- TECHNICAL PUBLICATION. Reports of completed research or a major significant phase of research that present the results of NASA programs and include extensive data or theoretical analysis. Includes compilations of significant scientific and technical data and information deemed to be of continuing reference value. NASA counterpart of peer-reviewed formal professional papers but has less stringent limitations on manuscript length and extent of graphic presentations.

- TECHNICAL MEMORANDUM. Scientific and technical findings that are preliminary or of specialized interest, e.g., quick release reports, working papers, and bibliographies that contain minimal annotation. Does not contain extensive analysis.

- CONTRACTOR REPORT. Scientific and technical findings by NASA-sponsored contractors and grantees.

- CONFERENCE PUBLICATION. Collected papers from scientific and technical conferences, symposia, seminars, or other meetings sponsored or cosponsored by NASA.

- SPECIAL PUBLICATION. Scientific, technical, or historical information from NASA programs, projects, and missions, often concerned with subjects having substantial public interest.

- TECHNICAL TRANSLATION. English-language translations of foreign scientific and technical material pertinent to NASA's mission.

Specialized services also include creating custom thesauri, building customized databases, organizing and publishing research results.

For more information about the NASA STI program, see the following:

- Access the NASA STI program home page at *http://www.sti.nasa.gov*

- E-mail your question to *help@sti.nasa.gov*

- Fax your question to the NASA STI Information Desk at 443–757–5803

- Phone the NASA STI Information Desk at 443–757–5802

- Write to:
  STI Information Desk
  NASA Center for AeroSpace Information
  7115 Standard Drive
  Hanover, MD 21076–1320

NASA/TM—2013-216547

Simulating the Use of Alternative Fuels in a Turbofan Engine

Jonathan S. Litt and Jeffrey C. Chin
Glenn Research Center, Cleveland, Ohio

Yuan Liu
N&R Engineering, Inc., Parma Heights, Ohio

National Aeronautics and
Space Administration

Glenn Research Center
Cleveland, Ohio 44135

September 2013

Acknowledgments

The authors wish to thank Jeffrey T. Csank, Ryan D. May, Thomas M. Lavelle, Christopher A. Snyder, Dean K. Frederick, and Zachary O. Baker for their gracious help and guidance. This work was sponsored by the Aviation Safety Program at the NASA Glenn Research Center.

Level of Review: This material has been technically reviewed by technical management.

Available from

NASA Center for Aerospace Information
7115 Standard Drive
Hanover, MD 21076–1320

National Technical Information Service
5301 Shawnee Road
Alexandria, VA 22312

Available electronically at http://www.sti.nasa.gov

Simulating the Use of Alternative Fuels in a Turbofan Engine

Jonathan S. Litt and Jeffrey C. Chin
National Aeronautics and Space Administration
Glenn Research Center
Cleveland, Ohio 44135

Yuan Liu
N&R Engineering, Inc.
Parma Heights, Ohio 44130

Abstract

The interest in alternative fuels for aviation has created a need to evaluate their effect on engine performance. The use of dynamic turbofan engine simulations enables the comparative modeling of the performance of these fuels on a realistic test bed in terms of dynamic response and control compared to traditional fuels. The analysis of overall engine performance and response characteristics can lead to a determination of the practicality of using specific alternative fuels in commercial aircraft. This paper describes a procedure to model the use of alternative fuels in a large commercial turbofan engine, and quantifies their effects on engine and vehicle performance. In addition, the modeling effort notionally demonstrates that engine performance may be maintained by modifying engine control system software parameters to account for the alternative fuel.

Nomenclature

ASTM	American Society for Testing and Materials
C_D	Drag force coefficient in the x direction
C_L	Lift force coefficient in the y direction
C_P	Heat capacity
EPR	Engine pressure ratio
FAR	Fuel-to-air ratio
g	Gravitational constant
LHV	Lower Heating Value
P30	High pressure compressor exit pressure
S	Wing planform area
T40	Burner exit temperature
T50	Low pressure turbine exit temperature
TSFC	Thrust specific fuel consumption
v	Velocity
W	Weight
W_i	Takeoff weight
W_f	Landing weight
x	Range
γ	Adiabatic index
ρ	Air density

Introduction

The worldwide interest in alternative energy is quickly gaining momentum as a result of political and socioeconomic concerns regarding the use of fossil fuels. The sheer magnitude of energy demand, in combination with sustainability and detrimental environmental effects of fossil fuels, makes the transition to alternative energy sources particularly attractive. The airline industry is responsible for 2 percent of annual global man-made CO_2 emissions (Ref. 1) and there is a growing awareness that the use of alternative jet fuels could produce a net reduction in these flight-related carbon emissions. Significant reduction has already been demonstrated in tests utilizing fuel blends and pure biofuels in unmodified engines (Refs. 2 to 4). Biofuels are emerging as a popular alternative energy source because of their renewability and potential to mitigate fossil fuel dependence.

Substituting aviation fuel is challenging, and stringent specifications set by the American Society for Testing and Materials (ASTM) help define that challenge. In addition to meeting tight quality standards, the fuel must serve multiple purposes within the engine. It is used as a hydraulic fluid in servo valves (Ref. 5), as a lubricant for valves and bearings, and as a coolant, which requires high thermal stability. Furthermore, standard fuels contain additives such as antioxidants and antistatic agents that prevent oxidation and static electricity generation, respectively, as well as corrosion and icing inhibitors.

Biodiesel is an alternative fuel that can be acquired through the transesterification of vegetable oils, used cooking oils, and animal fats. Production and use of biodiesel has increased worldwide because of its compatibility with existing fuel distribution and storage infrastructures. Advantages of biodiesels include reduced exhaust emissions, improved biodegradability, higher flash point, and domestic origin, but developmental hurdles include oxidative stability and cold flow properties (Ref. 6). There are methods to overcome some of these drawbacks using secondary treatments such as hydrogenation. This process removes oxygen from the biodiesel, resulting in a kerosene fuel with a greatly improved freezing point.

The growing interest in alternative fuels for aviation has created a demand to analyze the ramifications of their use. The availability of realistic dynamic turbofan engine simulations provides a way to evaluate these fuels from a propulsion system performance perspective. The introduction of the NASA-developed Modular Aero-Propulsion System Simulation (MAPSS) (Refs. 7 and 8), the Commercial Modular Aero-Propulsion System Simulation (C-MAPSS) (Refs. 9 to 11), and the Commercial Modular Aero-Propulsion System Simulation 40k (C-MAPSS40k) (Refs. 12 and 13) into the aerospace community has been a catalyst for research in diagnostics, prognostics, and control design for propulsion systems. Researchers are benefitting from the built-in capabilities and user-friendly features of these simulations that make them well-suited for controls and diagnostics algorithm development. However, these simulations were designed with specific uses in mind, and thus have limited capabilities outside of their preconceived domain. Still, the overall usefulness of the simulations has encouraged users to build on the baseline models to provide relevant features for their specific needs. Such features as compressor instability indication modeling, (Ref. 14) emissions modeling, (Ref. 15) and engine icing modeling (Ref. 16) are examples.

This paper lays out a procedure for modifying the C-MAPSS40k model to allow the simulation of the use of alternative fuels that do not require the physical modification of the fuel system. Specifically, the thermodynamic equations that incorporate the use of standard jet fuel implicitly are replaced by equivalent lookup tables. The lookup tables themselves can be swapped out for others that represent properties of different fuels, thus enabling the simulation of any desired fuel. Note that because of the modularity of the simulations and because the source code is accessible and can be modified, a user can replace the fuel pump model, for example, if desired (Ref. 12). Reference 17 describes actual fuel system hardware and control software modified for use with hydrogen fuel. The fuel properties may affect the engine performance and operation, the impact of which can be evaluated through simulation. In some cases, baseline performance can be recovered through controller gain modification, as this paper will demonstrate.

This paper is organized as follows. First, a modeling approach to enable the use of alternative fuels and the validation method are described. Next, the result of using such fuels on engine performance is demonstrated. This is followed by a sample analysis of the impact of using an example alternative fuel on

aircraft performance. The paper concludes with some final comments regarding the use of alternative fuels beyond what is capable of being simulated in the turbofan engine model utilized here and a summary of results.

Modeling Approach and Validation

C-MAPSS40k is a faster-than-real-time, zero-dimensional (lumped parameter) simulation of a 40,000 lbf thrust class engine that accurately models the engine dynamics to the fidelity appropriate for control system design. It has three inputs: fuel flow rate, variable stator vane (VSV) position, and variable bleed valve (VBV) position. It includes a realistic controller and enables the user to set initial and time-varying inputs to an engine operating in any part of the flight envelope. The engine model has been designed to be modular at a component level to allow for specific engine customization, which makes it a flexible platform that can be utilized for multi-disciplinary research. In this context, C-MAPSS40k should be able to accommodate the turbine engine's system performance considerations involving the next generation of fuels. Since C-MAPSS40k represents a generic commercial turbofan engine, only "drop-in" fuels that do not require significantly redesigned engines can be analyzed using this simulation as is, although modification of the simulation is possible.

Mechanical Fuel Properties: C-MAPSS40k models the physical combustion process using a 40-ms delay, combined with an efficiency parameter that encompasses minor resistances and losses at the liner and the mixer. When simulating the use of alternative fuel, it is assumed that any operational design issues regarding freezing, engine deposits and mixing are completely resolved. Biofuels have large carbon chain lengths and the presence of oxygen and fatty compounds result in higher kinematic viscosities than hydrocarbons of equal carbon length (Ref. 18). Additional differences can be found in Table 1.

Thermodynamic Fuel Properties: C-MAPSS40k utilizes a Lower Heating Value (LHV) parameter and a set of four thermodynamic functions to calculate the thermodynamic properties of the gas within the engine components. The LHV parameter, which resides in the burner component, is defined as the net amount of heat released by combusting a specific amount of fuel. The thermodynamic functions, which are utilized by all of the major engine components, relate certain gas properties given a specific fuel-air mixture level: two are used to convert between temperature and enthalpy; the other two functions convert between temperature and entropy, given pressure. The LHV and thermodynamic functions in the baseline C-MAPSS40k correspond to Jet-A, a standard aviation fuel.

The fuel's chemical composition, including the carbon-to-hydrogen ratio and molecular weight, factor into the mixture's heat capacity (C_P) and adiabatic index (γ), which in turn affect engine performance. Both the LHV parameter and the set of thermodynamic functions are fuel-specific and hence must be replaced when simulating other fuel types. Since the thermodynamic functions included in C-MAPSS40k are in a format that is not particularly amenable to user modification, the functions are replaced with two multi-dimensional arrays that explicitly relate the necessary thermodynamic properties: (1) a two-dimensional array of enthalpy values based on temperature and fuel-to-air ratio (FAR), and

TABLE 1.—KEY DIFFERENCES BETWEEN FUEL TYPES

Fuel properties	Standard Jet-A	Biodiesel, ethanol	Biodiesel, ethyl stearate
LHV (BTU/lb)	18,400	11,587	16,250
Kinematic viscosity (mm^2/sec)	1.39	1.07	3.7-5.8
Average density (lb/gal)	6.84	6.58	7.3
FAR (Stoichiometric)	0.068	0.111	0.074
Freezing point (°C)	−40	−114	−15
Generalized chemical composition	$C_{10}H_{19}$	C_2H_5OH	$C_{19}H_{38}O_2$
Average H/C ratio	1.9	3	2
Total molecular weight of combustion products at a FAR = 0.02 (g/mol)	28.968	28.820	29.197

(2) a three-dimensional array of entropy values based on temperature, pressure, and FAR. Two-dimensional and three-dimensional interpolation routines are used to traverse the arrays. The "inverse" relationships (i.e., enthalpy and FAR to temperature; entropy, pressure, and FAR to temperature) are calculated by applying the Newton-Raphson Method to the "forward" relationships (e.g., temperature to enthalpy). A thermodynamics software application is necessary to generate these arrays for different fuel types. For this work, the aforementioned enthalpy and entropy relationships were calculated using the *Chemical Equilibrium with Applications* (CEA) computer program (Ref. 19). The CEA program computes chemical equilibrium product concentrations from a given set of reactants and determines thermodynamic and transport properties for the product mixture. Since CEA accounts for the energy released due to combustion, the usage of LHV in the combustor model of C-MAPSS40k is redundant and removed when applying CEA-generated thermodynamic arrays.

As a preliminary study, one can get a general idea of the effects of using different fuels with C-MAPSS40k through some simpler changes. Adjusting LHV to match that of the fuel type and, if running open loop, scaling fuel flow to achieve the FAR required to meet the thrust demand (the controller will adjust fuel flow automatically in closed-loop operation) should be sufficient model modifications. However, more detailed comparisons of fuels will require replacing the default C-MAPSS40k thermodynamic relationships, as outlined above.

Validation: Utilizing multi-dimensional thermodynamic arrays to model different fuel types requires validation of (1) the interpolation routines and (2) the array generation procedure. First, to isolate the effects of interpolation, a nested-loop algorithm that repeatedly executes the original thermodynamic functions included in C-MAPSS40k was used to generate a 657-element two-dimensional array of enthalpy values and a 26,280-element three-dimensional array of entropy values. The performance of each major engine component using the original thermodynamic functions is then compared to that using array interpolation by applying the same inputs to the components (e.g., inlet pressure, temperature, mass flow rate) in both cases. The test case used for comparison corresponded to an operating condition of 1000 ft altitude and Mach 0.2. The percent differences observed in relevant output parameters obtained using interpolation relative to those obtained with the original thermodynamic functions are shown in the "Interpolation Only" column of Table 2. The results show that the differences introduced by interpolation are relatively small. The discrepancies may be attributed to the tolerance of the interpolation algorithms and the size of the arrays, the latter of which is balanced against model execution speed and computer memory considerations. The accuracy of the results can be improved as desired by increasing the size of the tables.

TABLE 2.—DIFFERENCES IN PRESSURE, TEMPERATURE, AND TORQUE BETWEEN THE BASELINE AND MODIFIED C-MAPSS40k FOR EACH MAJOR COMPONENT

Component	Parameter	Interpolation only, percent	Jet-A CEA maps, percent
Fan	Pressure	0	0
	Temperature	0.23	0.22
	Torque	1.96	1.80
LPC	Pressure	0	0
	Temperature	0.083	0.081
	Torque	0.41	0.46
HPC	Pressure	0	0
	Temperature	0.42	0.39
	Torque	0.83	0.81
Burner	Pressure	0	0
	Temperature	0.0014	0.55
HPT	Pressure	0.16	0.44
	Temperature	0.00034	0.26
	Torque	0.00019	0.032
LPT	Pressure	2.89	2.90
	Temperature	0.0088	0.42
	Torque	0.48	0.48

Next, the thermodynamic arrays generated using the CEA computer program were investigated. To ensure their consistency with the default C-MAPSS40k thermodynamic relationships, the previously described procedure for validating the interpolation routines was repeated for identically sized enthalpy and entropy arrays generated using CEA. As before, engine component performance using the arrays was compared to that using the original thermodynamic functions. The results, listed in the "Jet-A CEA Maps" column of Table 2, show that the discrepancies introduced by using CEA are relatively small and on the order of interpolation errors for several performance parameters. Nevertheless, to control for these differences and prevent possible ambiguity due to error "compounding" when performing a full engine analysis, any reference in the remainder of the paper to engine performance using Jet-A fuel implies the usage of CEA-generated Jet-A arrays (as opposed to the original thermodynamic functions). The results, listed in the "Jet-A CEA Maps" column of Table 2, show that the discrepancies introduced by using CEA are relatively small and on the order of interpolation errors for several performance parameters. Nevertheless, to control for these differences and prevent possible ambiguity due to error "compounding" when performing a full engine analysis, any reference in the remainder of the paper to engine performance using Jet-A fuel implies the usage of CEA-generated Jet-A arrays (as opposed to the original thermodynamic functions).

Effects of Different Fuels on Engine Outputs

The impact on engine response as a result of using an alternative fuel with relatively low combustion energy is demonstrated in this section to emphasize the difference the type of fuel can make on engine performance. The C-MAPSS40k simulation with its baseline full-envelope controller was modified as described above to utilize thermodynamic tables. It was then used to simulate the response to a throttle doublet (5° step up, 10° step down, 5° step up) using both ethanol and Jet-A, at an operating point of 1000 ft altitude and Mach 0.2. Figure 1 shows the engine pressure ratio (EPR) response for the two cases.

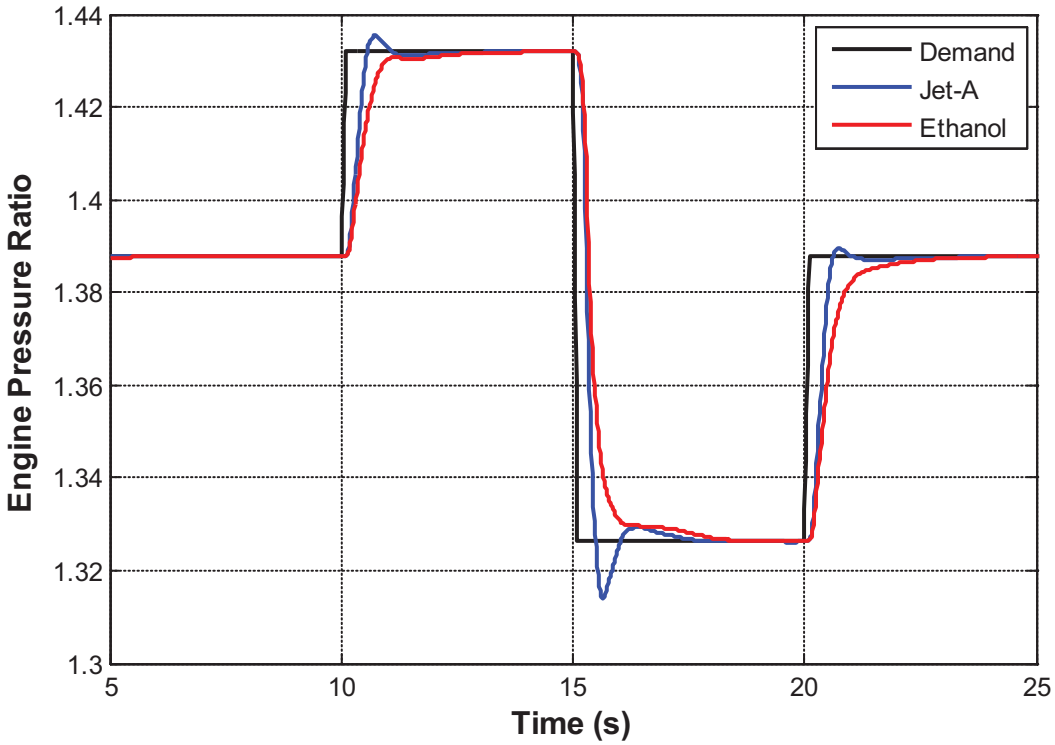

Figure 1.—EPR response to a doublet command in throttle (±5° about 70°) to C-MAPSS40k with its baseline controller, using Jet-A and Ethanol.

Ethanol's Lower Heating Value (LHV) of 11,587 BTU/lb is significantly lower than that for Jet-A (18,400 BTU/lb from Table 1). As a result, the response time of the engine using ethanol is somewhat slower. However, while this result can be partially attributed to fuel properties, it is also due to using a controller with gains designed for a fuel type with more combustion energy.

Thus, a redesign of the controller gains may result in recovery of the performance lost by using ethanol instead of Jet-A. To test this, linear models of the C-MAPSS40k engine using Jet-A and ethanol were first generated. The linearization routine in the baseline version of C-MAPSS40k utilizes a C-code version of the engine model with its default fuel properties, so it was modified to call the Simulink engine model[1] instead in order to account for the Jet-A- or ethanol-specific thermodynamic arrays. A model-matching linear regulator design (Ref. 20) tool available in C-MAPSS (Refs. 9 and 11) was then used to create EPR point controllers for the two linear models. The same design parameters (closed loop system specifications) were used for both controllers; these design parameters were selected to give approximately the same response as the full-envelope baseline controller at the design point. Figure 2 shows the response to a doublet input of the nonlinear engine model using the newly designed linear EPR point controllers. The Jet-A-powered engine with the EPR controller designed using the Jet-A linear model (blue line) is the baseline case. The Jet-A EPR controller used with an ethanol-powered engine (red line) results in slower engine response. However, by implementing a new linear EPR point controller designed using the ethanol linear model, the ethanol-powered engine (dashed green line) is able to match the Jet-A performance. The lower portion of Figure 2 shows the fuel flow corresponding to these redesigned EPR controller test cases. While the difference in transient response between fuel type can be accommodated by controller redesign, the ethanol-powered engine requires more than 60 percent higher fuel flow[2] to generate the same EPR as an engine using Jet-A. This is a result of the difference in energy content between the fuel types, and has implications for aircraft weight and range, which will be discussed later.

Modern commercial engines are designed to operate lean, i.e., the FAR is well below its stoichiometric ratio, or the ratio at which the products and reactants are balanced at a molecular level in a completely combusted reaction. This provides several advantages that were not modeled, but led to the decision to compare fuels at a lean design point. Operating lean can reduce NOx formation, increase fuel efficiency, and reduce combustor weight. It also reduces the chance of blade degradation and increased pollution caused by unburned hydrocarbons traveling downstream of the combustor. Additionally, operating with a FAR closer to stoichiometric results in excessive heat in the burner, which can also cause damage to the turbine blades. One advantage of using a fuel with a low LHV is that it burns at a lower temperature, even at the design FAR. Figure 3 shows the temperature of the hot gas entering the High Pressure Turbine (HPT) from the combustor. The HPT inlet temperature is over 50 °R cooler for the ethanol-powered engine, with the maximum difference at the peaks of nearly 65 °R lower. This can significantly extend the life of the components downstream of the combustor, particularly the HPT blades. It must be noted, however, that the higher fuel flow requirement of ethanol carries a weight penalty not only in fuel but potentially in the size of overall fuel system.

So far, analysis was conducted comparing propulsion system control performance for standard Jet-A fuel with ethanol. The subsequent analyses compare Jet-A to Ethyl Stearate, a biofuel that matches it more closely in terms of thermodynamic properties. Ethyl Stearate was chosen in particular, due to its similarities in molecular composition and heating value. Both fuels contain long carbon chains with

[1]It is anticipated that the ability to use the Simulink version of C-MAPSS40k to generate a linear model will be an option in future releases of C-MAPSS40k.

[2]In C-MAPSS40k, the fuel flow is measured in lb/sec, with the upper limit of 4.557 lb/sec. For Jet-A, this corresponds to about 0.666 gal/sec using the density of 6.84 lb/gal given in Table 1, which is the true limiting quantity. Since the density of ethanol is about 6.58 lb/gal, the mass flow limit of ethanol would be about 4.38 lb/sec. The peak fuel flow rate of ethanol in the doublet shown in Figure 2 is 4.505 lb/sec, so when modeling its use, a larger fuel metering valve would have to be assumed, although it does not limit by mass flow rate as in the current implementation.

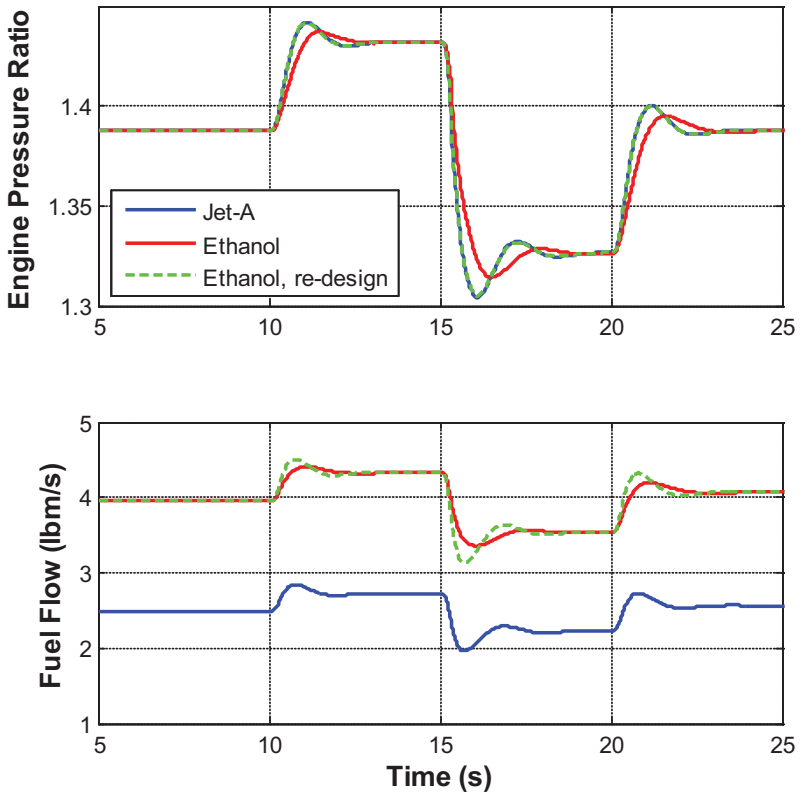

Figure 2.—Comparison of EPR response to a doublet in throttle for an engine using ethanol and an engine using Jet-A. The plots show EPR and corresponding fuel flow for a version of C-MAPSS40k with Jet-A (blue) and one with ethanol (red), using a point controller designed for Jet-A fuel. A third trace (dashed green) shows the same variables from C-MAPSS40k using ethanol, but with a redesigned point controller to match the Jet-A response.

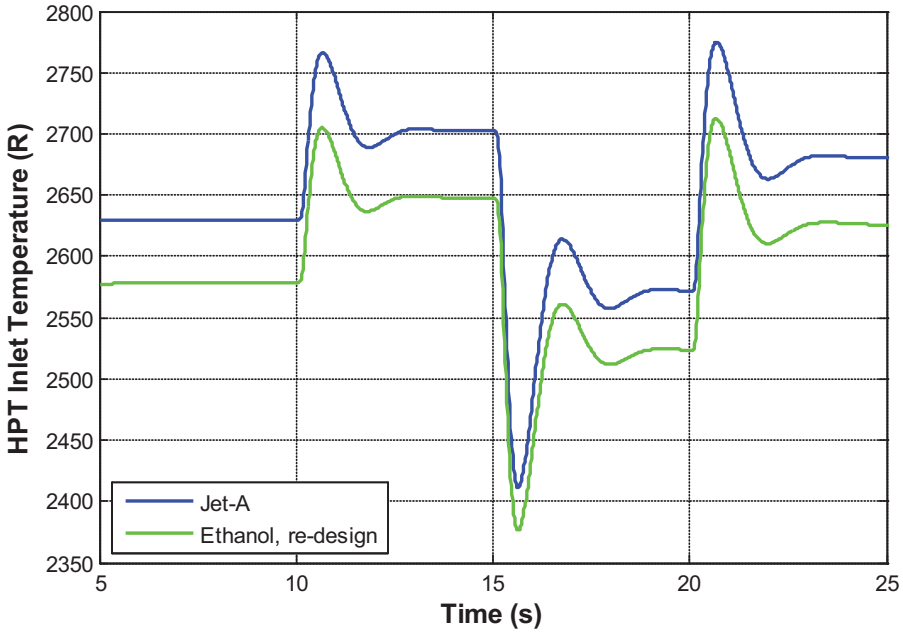

Figure 3.—Temperature at the inlet to the HPT for the doublet shown in Figure 2. For this transient, the temperature of the ethanol engine averages over 50 °R lower than that of the Jet-A engine for the same EPR.

similar hydrogen-to-carbon ratios, which indicate similar energy densities. Furthermore, the total molecular weights of their products after combustion differ by less than 0.8 percent when compared at a FAR of 0.02 using the chemical formulas listed in Table 1. This results in very similar heat capacities (C_P) and adiabatic indices (γ), which consequently affects turbine flow and overall Brayton cycle efficiency.

The thermodynamic tables for ethyl stearate were created using CEA and inserted into the modified version of C-MAPSS40k with its baseline controller. A simulated doublet in PLA was used as input at an operating point of 1000 ft altitude and Mach 0.2; the results are shown in Figure 4 and Figure 5. The biodiesel-powered engine responses shown (EPR, net thrust, T40, T50, P30) closely match those of the engine powered with standard fuel, but with a slight damping effect. The fuel flow for the biodiesel is about 15 percent higher than for Jet-A to produce the same EPR, due to the lower combustion energy of the fuel, but it is significantly lower than that required by ethanol (Figure 2). The burner exit temperature (T40) is slightly higher for Jet-A since its LHV is higher. The low pressure turbine exit temperature (T50) also has this characteristic. Ethyl stearate's lower peak temperatures are a result of using the baseline controller designed for use with Jet-A, not necessarily because of the different fuel properties.

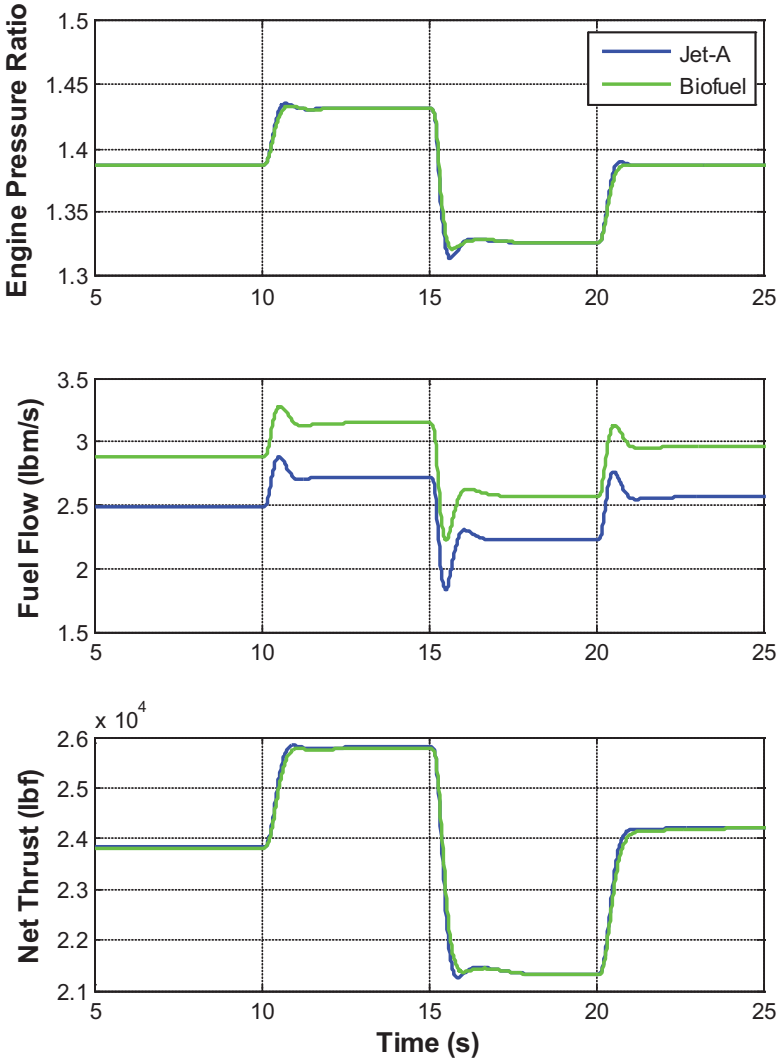

Figure 4.—Comparison of EPR, fuel flow, and net thrust responses for versions of C-MAPSS40k using Ethyl Stearate and Jet-A to a throttle doublet.

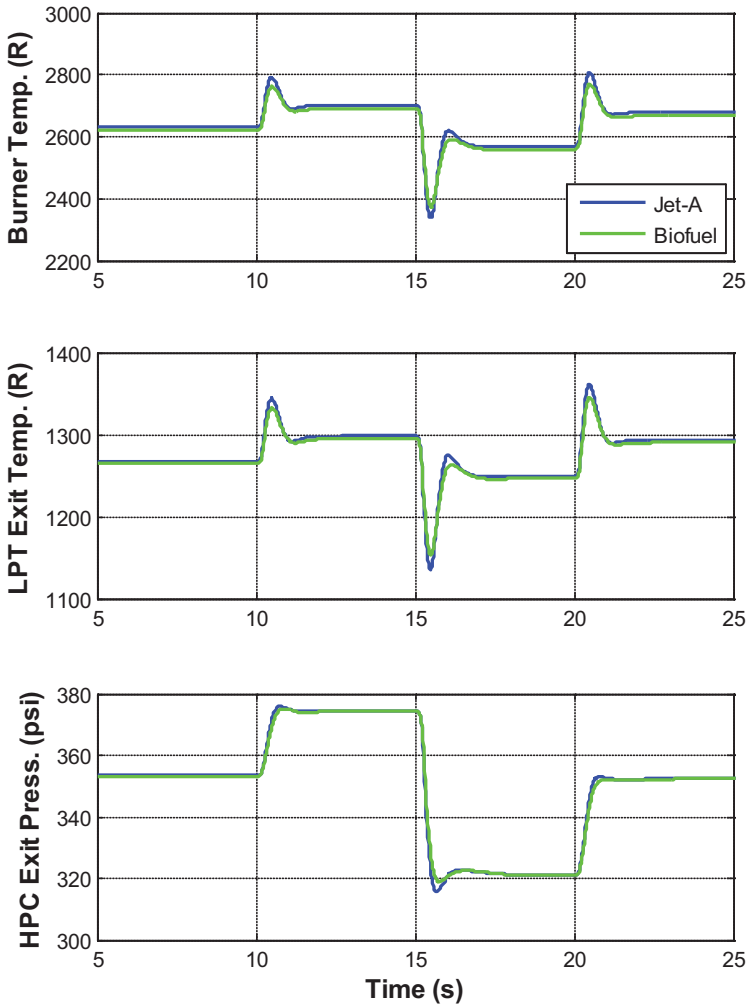

Figure 5.—Comparison of burner temperature (T40), LPT exit temperature (T50), and HPC exit pressure (P30) responses for versions of C-MAPSS40k using ethyl stearate and Jet-A to a throttle doublet.

Fuel Consumption Impact

In this section, a sample analysis of the effect of using the various fuels is performed in terms of their impact on aircraft operating range. The top plot of Figure 6 shows the difference in fuel flow rate for Jet-A and ethyl stearate corresponding to the case shown in Figure 4, which was covered in the previous section. The difference in fuel flow rate between the two fuel types increases and decreases with the actual fuel flow level. This means that fuel consumption is proportionally related. This becomes especially apparent in the bottom plot of Figure 6, which shows the cumulative fuel used over time. Biodiesel requires approximately 15 percent more fuel by weight, when compared in steady state. This makes sense since the biofuel has a lower heat of combustion, i.e., it has less energy per pound of fuel.

Using fuel flow and thrust data, it is possible to calculate thrust specific fuel consumption (TSFC) as

$$\mathrm{TSFC} = \frac{\text{fuel flow}}{\text{thrust}} \tag{1}$$

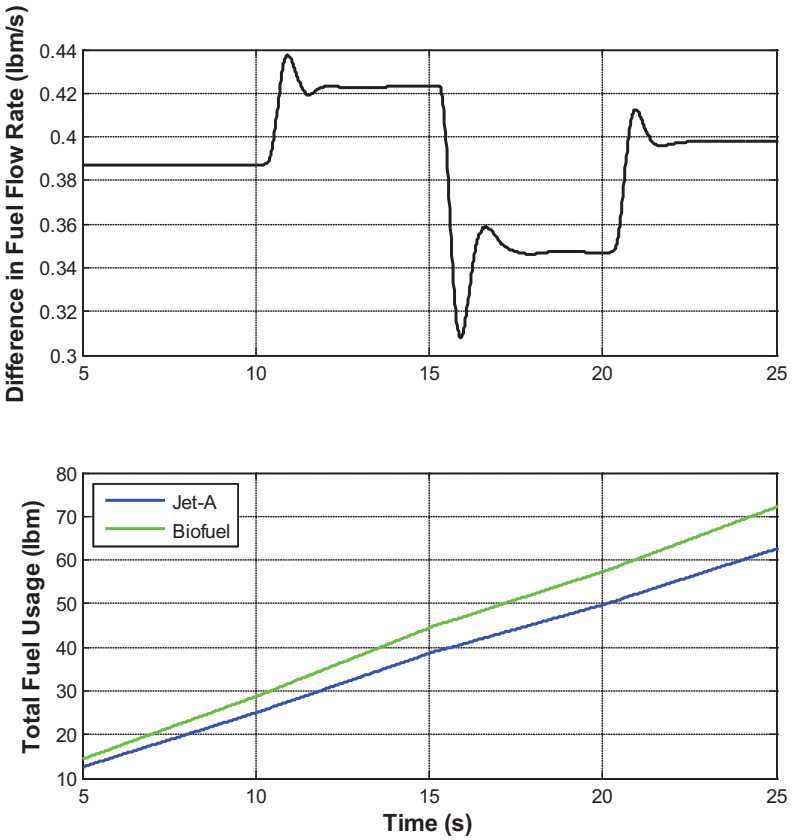

Figure 6.—Instantaneous difference in fuel flow rate (top) and total fuel usage (bottom) for the engine using Jet-A and the engine using biofuel, for the doublet shown in Figure 4.

With TSFC and the initial/final vehicle weight ratio, $\frac{W_i}{W_f}$, the aircraft range can be approximated, assuming constant velocity and lift coefficient (Ref. 21). The coefficients of lift and drag are defined as:

$$C_L = \frac{\text{Lift}}{\frac{1}{2}\rho v^2 S} \tag{2}$$

$$C_D = \frac{\text{Drag}}{\frac{1}{2}\rho v^2 S} \tag{3}$$

where ρ is the air density, v is the velocity, and S is the wing planform area. Since airplane weight decreases when fuel is consumed, one can develop the following range equation as a function of weight (Ref. 22).

$$\text{Range}, x = \left(\frac{v}{g}\right)\left(\frac{1}{\text{TSFC}}\right)\left(\frac{C_L}{C_D}\right)\ln\left(\frac{W_i}{W_f}\right) \tag{4}$$

This equation is known as the Breguet Equation. Equation (4) can be applied to two identical aircraft, one with Jet-A and one with biofuel (ethyl stearate). Assuming they travel the same distance, the Breguet Equations for the two aircraft can be equated (assume that all fuel is consumed so that the final weight, W_f, is also the empty weight and therefore is the same for both aircraft):

$$\left(\frac{1}{\mathrm{TSFC}_{\mathrm{biofuel}}}\right)\ln\left(\frac{W_{i,\mathrm{biofuel}}}{W_f}\right)=\left(\frac{1}{\mathrm{TSFC}_{\mathrm{Jet\text{-}A}}}\right)\ln\left(\frac{W_{i,\mathrm{Jet\text{-}A}}}{W_f}\right) \tag{5}$$

By rearranging Equation (5), the importance of the thrust specific fuel consumption becomes apparent.

$$\frac{W_{i,\mathrm{Jet\text{-}A}}}{W_f}=\left(\frac{W_{i,\mathrm{biofuel}}}{W_f}\right)^{\left(\frac{\mathrm{TSFC}_{\mathrm{Jet\text{-}A}}}{\mathrm{TSFC}_{\mathrm{biofuel}}}\right)} \tag{6}$$

An aircraft using biofuel will require more fuel as long as it has a higher TSFC, since the energy content is lower. In an attempt to reason why the difference in weight is governed by a power law, consider that the biofuel engine will consume fuel at a faster rate because of its lower energy density. Therefore, it needs to carry more fuel to travel the same distance, making the aircraft heavier. With a heavier aircraft, more fuel will be needed to generate enough lift. This compounding relationship results in the nonlinear relationship in fuel requirements. A longer flight necessitates a heavier biofuel tank and greater divergence between required amounts of fuel. To put this relationship in economic terms, analysis was performed for the least efficient scenario (i.e., maximum range as allowed by fuel tank capacity) using a 757-300 aircraft with twin 40k pound thrust class engines. Assuming the vehicle is filled to its maximum take-off weight (272,500 lb) including its maximum fuel capacity (11,466 gal) of ethyl stearate, an equivalent aircraft with the same non-fuel payload running on standard fuel will only need 10,307 gal to reach the same range (gross take-off weight is different). Thus, at worst, an ethyl stearate-powered aircraft needs approximately 11.2 percent more fuel by volume. Following the same procedure, if these vehicles were flown at half the maximum range of the biodiesel aircraft, the one using standard fuel would need 4746 gal, and the ethyl stearate craft would need 5209 gal, or 9.8 percent more fuel. The difference in fuel required by the two aircraft decreases as the flight range is shortened.

Discussion

As the push to make the use of biofuels more pervasive in the airline industry continues, it is important to understand their broader impact. Engine performance simulations using C-MAPSS40k have demonstrated the thermodynamic compatibility of biodiesel with existing engines. Biofuel engines will be able to produce equal amounts of thrust compared to conventionally powered engines with the same transient responses if the fuel flow controller is redesigned. From a system perspective, the most detrimental properties of certain biofuels are volume, weight, and freezing point. The volume and weight of certain biofuels will unavoidably reduce efficiency. Mixing standard fuel and biofuel would help reduce some of the aforementioned issues. From a component perspective, biodiesel's higher viscosity could also lead to less desirable atomization characteristics, such as increased mean droplet size. Furthermore, ring sticking, injector coking, and injector deposit problems have all been known to lead to pump failure in biodiesel truck engines. A mix of biodiesel and standard fuel would optimize the properties while also alleviating fossil fuel dependency.

In spite of viscosity issues, it has been found that biodiesel actually causes *less* wear in ground vehicle diesel engines (Ref. 23). This has been attributed to biodiesel's high lubricity. A high lubricity means that biodiesel will be less corrosive, improving the life of fuel handling components. With all of

these considerations together, it is difficult to determine how long term engine life trends will change. Biodiesel's oxidation and engine deposit problems could mean that fuel system maintenance must occur more often. Conversely, the life of components downstream from the combustor may increase when using biofuels based on the lower combustion temperature, as shown in Figure 3. Incomplete combustion would also affect blade life. Testing actual engine rigs would be necessary to make accurate and conclusive engine life estimates.

Tradeoffs exist in all engineering considerations, and alternative energy is characterized by its substantial entry costs. Nonetheless, the benefits may eventually prove to exceed the operating expenses. Biodiesel is much cleaner burning than petroleum, releasing fewer particulates into the air. It also emits 60 percent less *net* CO_2 than petroleum-based fuels since it originates from carbon dioxide absorbing plants (Ref. 24). As the demand for biofuel grows, it is anticipated that more companies will enter the market, which can help drive prices to a competitive level.

Biofuels have been mostly associated with ground transportation; however advances in biofuel production technologies will make them more attractive to the aviation industry. The use of biofuels cannot completely replace fossil fuels, but they can be used most effectively in specialized niches such as short flights. Regardless of certain commercialization obstacles, simulations have confirmed that from a propulsion system performance perspective, biofuels are compatible with current turbofan engines.

Summary

A technique was outlined and demonstrated to model the use of alternative fuels in a nonlinear turbofan engine simulation to conduct propulsion system performance studies. The approach described here is specific to the engine simulation used—C-MAPSS40k—and the method used to generate the enthalpy and entropy tables corresponding to the type of fuel desired; however, the concepts are fairly general. The description is at a high level, but is sufficient to guide the experienced user. The results demonstrated the compatibility of biofuels with current turbofan engines from a propulsion system performance perspective. Even with a fuel such as ethanol, which has significantly lower energy content than standard jet fuel, simple controller gain modifications were shown to completely recover the engine response, albeit with a higher fuel flow rate. Therefore, the simulation modified to accept tables representing the properties of a variety of alternative fuels, can be used to evaluate the impact of using these fuels on thrust specific fuel consumption, temperatures, and other variables, and these in turn can be used to evaluate the impact on aircraft weight and range.

References

1. "Beginner's Guide to Aviation Biofuels," Air Transport Action Group. May 2009.URL: http://www.enviro.aero/Content/Upload/File/BeginnersGuide_Biofuels_WebRes.pdf. [Cited 6 April 2012].
2. Bulzan, Dan, et al., "Gaseous and Particulate Emissions Results of the NASA Alternative Aviation Fuel Experiment (AAFEX)," GT2010-23524, Proceedings of ASME Turbo Expo 2010: Power for Land, Sea and Air GT2010, June 14-18, 2010 Glasgow, Scotland.
3. Harrington, Kent, "Data Reveals First Civilian All-Biofuel Flight Was a Success," http://chenected.aiche.org/energy/data-reveals-first-civilian-all-biofuel-flight-was-a-success/ accessed April 30, 2013.
4. Vergakis, Brock, "NASA measures effects of jet engine biofuel," http://www.miamiherald.com/2013/04/25/3364625/nasa-measures-effects-of-jet-engine.html, accessed April 30, 2013.
5. Lawicki, David, "Jet Fuel Characteristics," *Smart Cockpit*. Boeing, Mar 2002. Web. 6 Apr 2010. http://www.smartcockpit.com/data/pdfs/flightops/aerodynamics/Jet_Fuel_Characteristics.pdf.
6. Daggett, D., O. Hadaller, R. Hendricks, and R. Walther, "Alternative Fuels and Their Potential Impact on Aviation," NASA/TM—2006-214365, October 2006.

7. Parker, K.I., Guo, T. -H., "Development of a Turbofan Engine Simulation in a Graphical Simulation Environment," NASA/TM—2003-212543, August 2003.
8. K.I. Parker, K.J. Melcher, "The Modular Aero-Propulsion System Simulation (MAPSS) Users' Guide," NASA TM—2004-212968, March 2004.
9. Frederick, Dean K., DeCastro, Jonathan A., Litt, Jonathan S., "User's Guide for the Commercial Modular Aero-Propulsion System Simulation (C-MAPSS)," NASA/TM—2007-215026, October 2007.
10. DeCastro, J.A., Litt, J.S., Frederick, D.K., "A Modular Aero-Propulsion System Simulation of a Large Commercial Aircraft Engine," AIAA-2008-4579, 44th AIAA/ASME/SAE/ASEE Joint Propulsion Conference & Exhibit, Hartford, CT, July 21-23, 2008, NASA/TM—2008-215303, September 2008.
11. Liu, Yuan; Frederick, Dean, K.; DeCastro, Jonathan, A.; Litt, Jonathan, S.; Chan, William, W., "User's Guide for the Commercial Modular Aero-Propulsion System Simulation (C-MAPSS) Version 2," NASA/TM—2012-217432, March 2012.
12. May, R.D., Csank, J., Lavelle, T.M., Litt, J.S., and Guo, T.-H., "A High-Fidelity Simulation of a Generic Commercial Aircraft Engine and Controller," AIAA-2010-6630, AIAA 46th Joint Propulsion Conference, Nashville, TN, July 25-28, 2010.
13. Csank, J., May, R.D., Litt, J.S., Guo, T.-H., "Control Design for a Generic Commercial Aircraft Engine," AIAA-2010-6629, AIAA 46th Joint Propulsion Conference, Nashville, TN, July 25-28, 2010.
14. Liu, Yuan, Dhingra, Manuj, Prasad, J.V.R., "Benefits of Active Compressor Stability Management on Turbofan Engine Operability," Journal of Engineering for Gas Turbines and Power, July 2009, vol. 131.
15. Cheng, Victor H.L., and Sweriduk, Gregory D., "Trajectory Design for Aircraft Taxi Automation to Benefit Trajectory-Based Operations," Proceedings of the 7th Asian Control Conference, Hong Kong, China, August 27-29, 2009.
16. May, R.D., Guo, T-H., Veres J.P., Jorgenson, P.C.E., "Engine Icing Modeling and Simulation (Part 2): Performance Simulation of Engine Rollback Phenomena," 2011-38-0026, SAE International Conference on Aircraft and Engine Icing and Ground Deicing, Chicago, IL, Jun 13-17, 2011.
17. Boerner, S., Funke, H.H.-W., Hendrick, P., Recker, E., "*Control System Modifications for a Hydrogen Fuelled Gas-Turbine*," The 13th International Symposium on Transport Phenomena and Dynamics of Rotating Machinery (ISROMAC-13), Honolulu, HI, April 4-7, 2010.
18. Knothe, Gerhard, and Steidley, Kevin, "Kinematic viscosity of biodiesel fuel components and related compounds. Influence of compound structure and comparison to petrodiesel fuel components," *Fuel: The Technology and Science of Fuel and Energy* 84 (2005), pp. 1059-1065.
19. Sanford Gordon and Bonnie J. McBride, "Computer Program for Calculation of Complex Chemical Equilibrium Compositions and Applications," NASA RP-1311, October 1994.
20. Edmunds, J.M., "Control System Design and Analysis Using Closed-Loop Nyquist and Bode Arrays," International Journal of Control, vol. 30, no. 5, 1979, pp. 773–802.
21. Farokhi, Saeed. *Aircraft Propulsion*. Hoboken, NJ: John Wiley & Sons, 2009.
22. Nygren, Kip, and Robert Schulz. "Breguet's Formulas for Aircraft Range & Endurance An Application of Integral Calculus," *United States Military Academy* 1996: n. pag. URL: http://mae.nmsu.edu/~aseemath/Schulz_96.PDF. [Cited 3 Mar 2010].
23. Argawal, A.K., J. Bijwe, and L.M. Das, "Effect of Biodiesel Utilization of Wear of Vital Parts in Compression Ignition Engine." Journal of Engineering for Gas Turbines and Power. vol. 125, issue 2, April 2003.
24. Bomani, Bilal, Dan Bulzan, Diana Centeno-Gomez, and Robert Hendricks. "Biofuels as an Alternative Energy Source for Aviation—A Survey," NASA/TM—2009-215587, December 2009.